

Articles

Combinatorial Study of the Optimization of $Y_2O_3:Bi,Eu$ Red Phosphors

Ting-Shan Chan,[†] Chia-Chen Kang,[†] Ru-Shi Liu,^{*,†} Lei Chen,[‡] Xiao-Nan Liu,[‡]
Jian-Jun Ding,[‡] Jun Bao,[‡] and Chen Gao[‡]

Department of Chemistry, National Taiwan University, Taipei 106, Taiwan, and National Synchrotron Radiation Laboratory and Structure Research Laboratory, University of Science & Technology of China, Hefei 230026, China

Received January 8, 2007

The present investigation aims at the synthesis of $(Y_{2-x}Eu_xBi_y)O_3$ red phosphor materials using the combinatorial chemistry method. We developed square-type arrays consisting of 90 compositions to obtain the optimum composition of co-dopants in a Y_2O_3 host. The optimized composition was found to be $(Y_{2-x}Eu_xBi_y)O_3$ ($x = 0.16–0.18$, $y = 0.08–0.10$). The screening of the compositions was investigated by analysis of the emission spectrum under 365 nm UV excitation arising from the energy transfer between Bi^{3+} and Eu^{3+} ions. The results of the photoluminescence excited by ultraviolet agree well with the conventional-scale synthesis results, indicating that the combinatorial screening method is fast, reliable, reproducible, and applicable to the study of powder materials with relatively quick calcinations at high synthesis temperatures.

Introduction

White light-emitting diodes (LEDs) have attracted interest because of their most challenging application as a replacement for conventional incandescent bulbs and fluorescent lamps.¹ It is generally accepted that white-light generation is likely to be achieved in one of two ways. First, blue, green, and red diodes can be combined to yield white light, and second, in a very cheap way, a single white LED can be obtained from the combination of an LED chip with phosphors. A device has been successfully developed, using the latter approach, by using YAG:Ce as a broadband yellow phosphor coated on a blue LED chip. However, this phosphor faces serious problems of thermal quenching, poor color rendition, and a narrow visible range. As an alternative, a novel approach has been suggested which uses a vacuum or near-UV excitation instead of a blue LED in combination with red, green, and blue phosphors to generate white LEDs.² Among the various red phosphors, Eu^{2+} -doped Y_2O_3 is considered to be the most promising candidate, compared with other sulfides,^{3–10} because of its chemical stability. Red phosphors $(Y_{1.84-y}Eu_{0.16}Bi_yO_3)$ ($0 < y \leq 0.12$) were synthesized by homogeneous coprecipitation and solid-state reactions in one of our previous investigations.¹¹ We found that the efficiency of the phosphor can be enhanced by energy transfer from Bi^{3+} to Eu^{3+} . These red phosphors could be

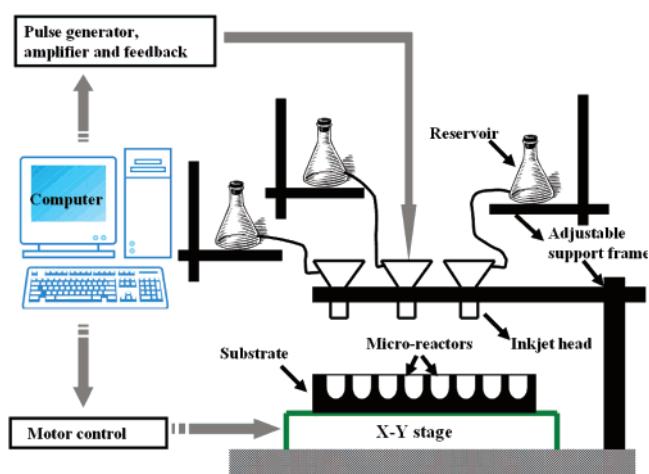


Figure 1. Schematic diagram of the drop-on-demand inkjet delivery system

excited by 350–400 nm UV light and used in white LEDs. It was observed that when the concentration of Bi^{3+} ions increased gradually, the lattice constant and color purity were increased because of the increased energy-transfer rate.

Recently, combinatorial chemistry has been widely applied to the synthesis of a variety of materials, such as drugs in pharmaceutical analysis or various inorganic functional materials.^{12–14} The use of a combinatorial approach will make it possible to search a fairly large phase space rapidly and exhaustively. The present investigation aims at the application of the liquid-state combinatorial chemistry method to the synthesis of phosphor materials. Combinatorial methods

* To whom correspondence should be addressed. E-mail: rslu@ntu.edu.tw.

[†] Department of Chemistry.

[‡] National Synchrotron Radiation Laboratory and Structural Research Laboratory.

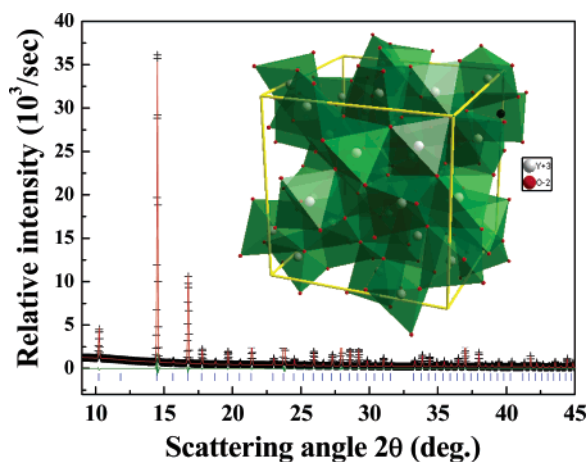


Figure 2. Observed (crosses), calculated (solid line), and differences (bottom) synchrotron XRD pattern of $(Y_{2-x}Eu_xBi_y)O_3$ ($x = 0.16$, $y = 0.16$) at 300 K with $\lambda = 0.7749$ Å. Bragg reflections are indicated by tick marks. An ideal crystal structure is also shown in the inset.

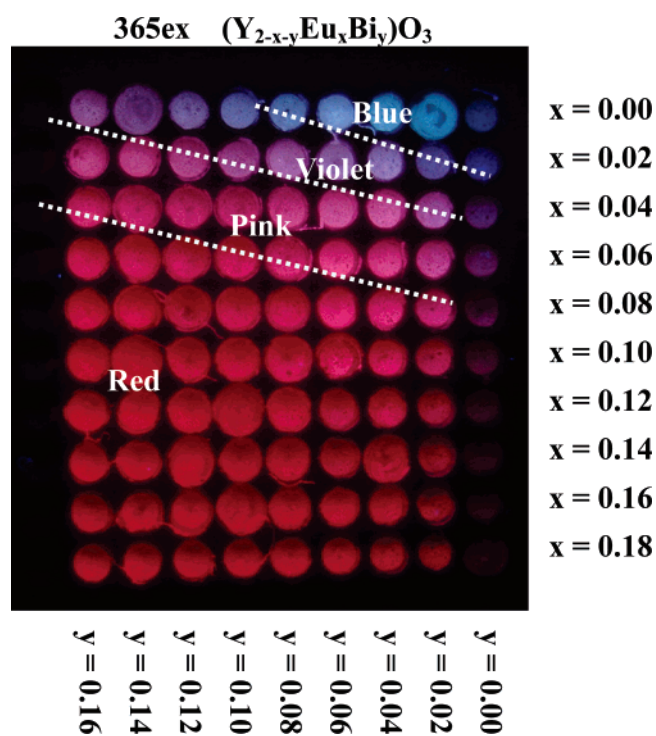


Figure 3. Composition map and photoluminescence photography of the library excited under 365 nm UV light for $(Y_{2-x}Eu_xBi_y)O_3$.

make it possible to rapidly synthesize, process, and analyze large libraries (with hundreds to thousands of members), dramatically accelerating the rate at which these experiments can be designed, executed, and analyzed. Thus, the aim of this article is to further investigate our previously reported work¹¹ on the optimization of $Y_2O_3:Bi$, Eu red phosphors using the combinatorial chemistry method. To the best of our knowledge, this is the first report to use a combinatorial chemistry method to study Eu^{3+} and Bi^{3+} ions co-doped efficiently in a Y_2O_3 host.

Experimental Section

The schematic diagram of the drop-on-demand inkjet delivery system developed is shown in Figure 1. The eight

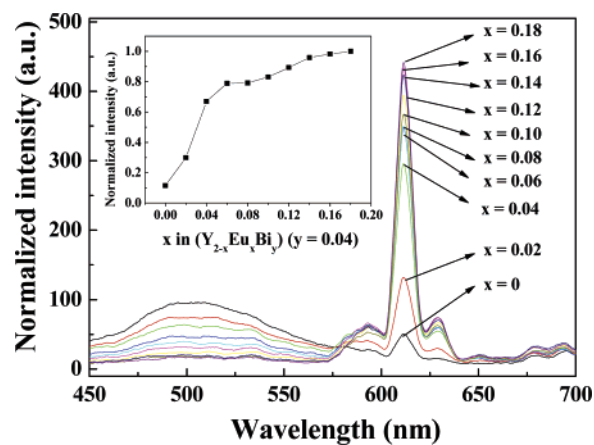


Figure 4. Emission spectrum of $(Y_{2-x}Eu_xBi_y)O_3$ ($y = 0.04$) with different Eu^{3+} contents. The normalized intensity as a function of x is also shown in the inset.

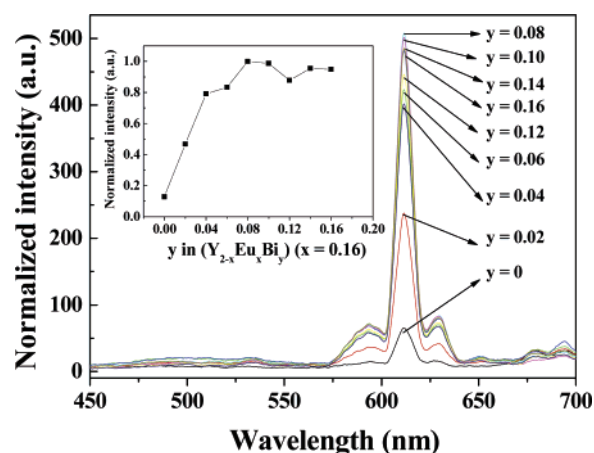


Figure 5. Emission spectrum of $(Y_{2-x}Eu_xBi_y)O_3$ ($x = 0.16$) with different Eu^{3+} contents. The normalized intensity as a function of y is also shown in the inset.

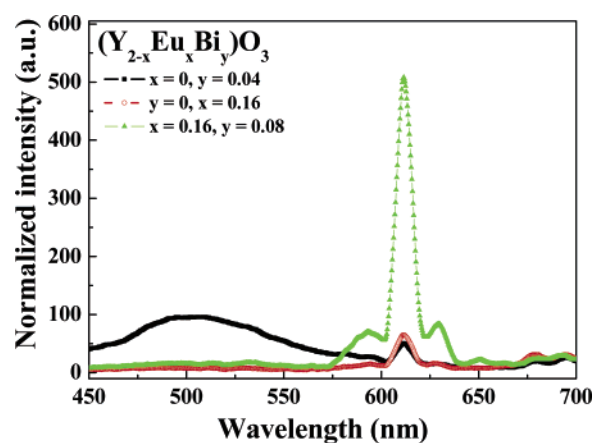


Figure 6. Emission spectrum of $(Y_{2-x}Eu_xBi_y)O_3$ ($x = 0$, $y = 0.04$), $(Y_{2-x}Eu_xBi_y)O_3$ ($x = 0.16$, $y = 0$), and $(Y_{2-x}Eu_xBi_y)O_3$ ($x = 0.16$, $y = 0.08$) phosphors measured under 365 nm UV excitation.

independent piezoelectric inkjet heads and the X–Y stage are controlled by the computer via the driving circuit and motor controller. Each inkjet head is connected to a suspension reservoir through a tube, and the substrate with a microreactor array is fixed on the stage. Moreover, the emission spectra of the samples in the library were measured using an automatic system. The main parts of the system

Table 1. Crystallographic Data for $(Y_{2-x}Eu_xBi_y)O_3$ ($x = 0.16, y = 0.16$) Phosphor, Constraints on Atomic Position, and U_{iso}^a

atoms	x	y	z	occupancy	U_{iso} (\AA^2)
Y(1)	0.25	0.25	0.25	0.84	2.89(6)
Eu(1)	0.25	0.25	0.25	0.08	2.89(6)
Bi(1)	0.25	0.25	0.25	0.08	2.89(6)
Y(2)	-0.0309 (6)	0	0.25	0.84	2.67(3)
Eu(2)	-0.0309 (6)	0	0.25	0.08	2.67(3)
Bi(2)	-0.0309 (6)	0	0.25	0.08	2.67(3)
O	0.3917(4)	0.1510 (5)	0.3807(4)	2.80(2)	2.80(2)

	reliability factors			interatomic distances (\AA)	
space group	$Ia\bar{3}$ (Cubic)	χ^2	0.68%	M(1)–M(1) ($\times 3$)	3.5506(4)
cell params	$a = b = c = 10.6822(9)$ \AA	R_p	1.82%	M(1)–M(1) ($\times 3$)	4.0174(5)
	$\alpha = \beta = \gamma = 90^\circ$	R_{wp}	3.11%	M(1)–M(2) ($\times 2$)	3.5493(4)
cell vol	$1218.93(2)$ \AA^3			M(1)–M(2) ($\times 2$)	4.0310(4)
				M(1)–O ($\times 2$)	2.2877(2)
				M(1)–O ($\times 2$)	2.3150(2)
				M(1)–O ($\times 2$)	2.3566(2)
				M(2)–O ($\times 2$)	2.2884(2)

^a Y = Eu = Bi; M = Y, Eu, and Bi.

consist of an Hg Lamp, a portable optical fiber spectrometer (Ocean Optics, Inc., model SD2000), and an X–Y stage. More details can be found in a previous report.¹⁵ With the aid of a homemade inkjet delivery system, precursors (>99.99% purity) such as 0.1 M $Y(NO_3)_3 \cdot 6(H_2O)$, 0.01 M Eu_2O_3 , and 0.01 M $Bi(NO_3)_3 \cdot 5(H_2O)$ were dissolved in nitric acid and deionized water. Then the correct amount of each solution was collected in an Al_2O_3 ceramic substrate according to the composition map with the assistance of a computer programmed inject system. The substrates containing the solutions were first dried at 100 °C for 1 h in an oven and then placed in an electric furnace where the temperature was slowly increased to 500 °C at the rate of 3 °C min^{-1} . Finally, the dried samples were pulverized and successively sintered at 1300 °C for 3 h in an ambient atmosphere.

Some of the chosen samples among those in the library were taken out of the Al_2O_3 ceramic substrate and then examined by synchrotron X-ray diffraction (XRD) analysis with a large Debye–Scherrer camera installed at the BL01C2 beam line at the National Synchrotron Radiation Research Center (NSRRC) in Taiwan. The synchrotron XRD data were collected in a 2θ range from 0.16 to 45° with a step interval of 0.01° and $\lambda = 0.7749$ \AA . The GSAS program¹⁶ was used for the Rietveld refinements to obtain information on the crystal structures of $(Y_{2-x}Eu_xBi_y)O_3$.

Results and Discussion

Figure 2 shows a typical example of matrix samples of the experimental, calculated, and difference synchrotron XRD patterns of $(Y_{2-x}Eu_xBi_y)O_3$ ($x = 0.16, y = 0.16$) at 300 K with $\lambda = 0.7749$ \AA . An ideal crystal structure is also shown in the inset. The observed peaks can be indexed on the basis of a cubic unit cell (space group $Ia\bar{3}$). However, we could not obtain the occupancy refinements for complex cation substitution because of the difficulty in using the X-ray powder diffraction data resulting from instrumental limits. Here, we assume that the Eu^{3+} and Bi^{3+} ions substituted into the Y^{3+} sites follow an ideal distribution. We therefore kept the values of occupancies constant for the (Y, Eu, Bi) sites in our data refinements. The final structural parameters and

selected bond lengths are given in Table 1. The atomic position of M(1) (M = Y, Eu, and Bi) corresponds to the 24d site with C_2 symmetry which does not have inversion symmetry, and the atomic position of M(2) (M = Y, Eu, and Bi) is the 8b site with S_6 symmetry which has inversion symmetry. As seen from Table 1, the final R factors of the refinement are $R_p = 1.82\%$, $R_{wp} = 3.11\%$, and $\chi = 0.86$ and the lattice constants are $a = b = c = 10.6822$ (9) \AA .

The composition map and luminescent photograph of the $(Y_{2-x}Eu_xBi_y)O_3$ library under 365 nm UV excitation are shown in Figure 3. The square-type arrays consist of 90 compositions with co-doped different Eu^{3+} contents from $x = 0$ to 0.18 and Bi^{3+} contents from $y = 0$ to 0.16. The lamp light was illuminated evenly over the library to obtain a relative comparison. It is apparent that the color change is from blue \rightarrow violet \rightarrow pink \rightarrow red with increasing Eu content.

Figure 4 presents the emission spectra of $(Y_{2-x}Eu_xBi_y)O_3$ ($y = 0.04$), which varies with the Eu^{3+} content in the library. The normalized intensity from $\lambda = 601$ –622 nm according to Figure 4 is also shown in the inset. When phosphors were excited under 365 nm, because of the energy transfer from Bi^{3+} to Eu^{3+} , Bi^{3+} acted as a sensitizer for Eu^{3+} emission, and these emission spectra consist of lines in the red region of the spectra corresponding to the transition from the excited 5D_0 to 7D_J ($J = 0, 1, 2, 3, 4$) of the Eu^{3+} ion.¹⁷ The most intense line at 612 nm corresponds to the hypersensitive transition between the 5D_0 to 7D_2 level of the Eu^{3+} ion. In addition, as can be seen in Figure 4, the intensity increased with increasing Eu^{3+} content, and the maximum intensity observed is for $x = 0.16$ –0.18, which is in good agreement with results using the traditional solid-state reaction method from one of our previous studies.¹¹ The result indicates that an appropriate amount of Eu^{3+} was properly doped into the Y_2O_3 matrix and formed homogeneous material in the library.

Figure 5 presents the emission spectra of $(Y_{2-x}Eu_xBi_y)O_3$ ($x = 0.16$), which varies with the Bi^{3+} content in the library. The normalized intensity from $\lambda = 601$ –622 nm according to Figure 5 is also shown in the inset. The concentration

quenching effect is clearly exhibited as evident from Figure 5, and the Bi^{3+} concentration of maximum intensity is found in $y = 0.08\text{--}0.10$, which is similar to the findings in one of our previous reports ($\text{Bi}^{3+} = 0.06$).¹¹ Therefore, the optimum composition was found to be $(\text{Y}_{2-x}\text{Eu}_x\text{Bi}_y)\text{O}_3$ ($x = 0.16\text{--}0.18$, $y = 0.08\text{--}0.10$) using the combinatorial chemistry method.

Figure 6 shows the emission spectra of $(\text{Y}_{2-x}\text{Eu}_x\text{Bi}_y)\text{O}_3$ ($x = 0$, $y = 0.04$), $(\text{Y}_{2-x}\text{Eu}_x\text{Bi}_y)\text{O}_3$ ($x = 0.16$, $y = 0$), and $(\text{Y}_{2-x}\text{Eu}_x\text{Bi}_y)\text{O}_3$ ($x = 0.16$, $y = 0.08$). It is well-known that the efficiency of the phosphor can be greatly enhanced by the energy transfer from the $^1\text{S}_0 \rightarrow ^3\text{P}_1$ transition of the Bi^{3+} ion to the Eu^{3+} ion.^{18–19} Here, we can get a good understanding of the energy transfer by comparing the three emission spectra. For $(\text{Y}_{2-x}\text{Eu}_x\text{Bi}_y)\text{O}_3$ ($x = 0$, $y = 0.04$), the broad peak located at about 450–550 nm was observed clearly and is caused by the blue-green light radiated by the Bi^{3+} ion. Thus, in the $(\text{Y}_{2-x}\text{Eu}_x\text{Bi}_y)\text{O}_3$ ($x = 0.16$, $y = 0$) sample, we did not find this phenomenon. Moreover, in the $(\text{Y}_{2-x}\text{Eu}_x\text{Bi}_y)\text{O}_3$ ($x = 0.16$, $y = 0.08$) sample, with Bi^{3+} concentration increased to $y = 0.08$, the most intense line at 612 nm was significantly increased. Such an observation could be key evidence for the effective energy transfer from Bi^{3+} to Eu^{3+} .

Conclusion

Red phosphors $(\text{Y}_{2-x}\text{Eu}_x\text{Bi}_y)\text{O}_3$ ($x = 0\text{--}0.18$, $y = 0\text{--}0.16$) have been synthesized using the combinatorial chemistry method. The optimum composition was found to be $(\text{Y}_{2-x}\text{Eu}_x\text{Bi}_y)\text{O}_3$ ($x = 0.16\text{--}0.18$, $y = 0.08\text{--}0.10$). On the basis of the above results, it is reasonable to believe that the developed combinatorial chemistry method makes the search process for a new oxide-based red phosphor for use in white LEDs possible.

Acknowledgment. We thank the National Science Council of Taiwan (Grant 95-2113-M-002-009) and the Ministry

of Economic Affairs of Taiwan (Grant 95-EC-17-A-078-S1-043) for financial support.

References and Notes

- (1) Nakamura, S.; Fasol, G. *The Blue Laser Diode: GaN Based Light Emitters and Lasers*; Springer: Heidelberg, Germany, 1997.
- (2) Shimizu, Y.; Sakano, K.; Noguchi, Y.; Moriguchi, T. U.S. Patent 5,998,925, 1999.
- (3) Ando, M.; Ono, Y. A. *J. Appl. Phys.* **1990**, *68*, 3578.
- (4) Pham-Thi, M. *J. Appl. Phys.* **1992**, *31*, 2811.
- (5) Yamashita, N. *J. Electrochem. Soc.* **1993**, *140*, 840.
- (6) Pham-Thi, M.; Ruelle, N.; Tronc, E.; Simons, D.; Vivien, D. *Jpn. J. Appl. Phys.* **1994**, *33*, 1876.
- (7) Luo, X.; Li, D. *SID Digest* **1992**, *92*, 175.
- (8) Swiatek, K.; Karpinska, K.; Godlewski, M.; Niinistö, L.; Leskelä, M. *J. Lumin.* **1994**, *60–61*, 923.
- (9) Choi, H.; Kim, C. H.; Pyun, C. H.; Kim, S. J. *J. Solid State Chem.* **1998**, *138*, 149.
- (10) Wu, J.; Newman, D.; Viney, I. V. F. *J. Lumin.* **2002**, *99*, 237.
- (11) Chi, L. S.; Liu, R. S.; Lee, B. J. *J. Electrochem. Soc.* **2005**, *152*, J93.
- (12) McFarland, E. W.; Weinberg, W. H. *Trends Biotechnol.* **1999**, *17*, 107.
- (13) Senkan, S. M. *Nature* **1998**, *394*, 350.
- (14) Xiang, X-D. *Ann. Rev. Mater. Sci.* **1999**, *29*, 149.
- (15) Chen, L.; Bao, J.; Gao, C. *J. Comb. Chem.* **2004**, *6*, 699.
- (16) Larson, A. C.; Von Dreele, R. B. *Generalized Structure Analysis System (GSAS)*; Los Alamos National Laboratory Report LAUR 86-748; Los Alamos National Laboratory: Los Alamos, NM, 1994.
- (17) Blasse, G.; Grabmaier, B. C.; *Luminescent Materials*; Springer: Berlin, 1994; p 117.
- (18) Li, B.; Sun, S. J. *Inorg. Mater.* **1993**, *8*, 207.
- (19) Datta, R. K. *J. Electrochem. Soc.* **1967**, *114*, 1137.

CC070006L